Article

Conceptual Recycling Chain for Proton Exchange Membrane Water Electrolyzer –Case Study Involving a Review Derived Model Stack

Malena Staudacher [*] , Dominik Goes , Sohyun Ahn , Dzeneta Vrucak , Tim Gießmann ,
Bernhard Bauer-Siebenlist , Thomas Leißner [*] , Martin Rudolph , Jürgen Fleischer , Bernd Friedrich ,
Urs A. Peuker

Article

Conceptual Recycling Chain for Proton Exchange Membrane Water Electrolyzer—Case Study Involving a Review Derived Model Stack

Malena Staudacher [1], Dominik Goes [2], Sohyun Ahn [3], Dzeneta Vrucak [4], Tim Gießmann [4], Bernhard Bauer-Siebenlist [5], Thomas Leißner [1,*], Martin Rudolph [3], Jürgen Fleischer [2], Bernd Friedrich [4] and Urs Peuker [1]

[1] TU Bergakademie Freiberg, Institute for Mechanical Process Engineering and Mineral Processing, Agricolastr. 1, 09599 Freiberg, Germany

[2] wbk Institute of Production Science, KIT Karlsruhe Institute of Technology, Kaiserstraße 12, Karlsruhe 76131, Germany

[3] Helmholtz-Zentrum Dresden-Rossendorf, Helmholtz Institute Freiberg for Resource Technology, Chemnitzer Straße 40, Freiberg 09599, Germany

[4] IME Process Metallurgy and Metal Recycling, RWTH Aachen University, 52056 Aachen, Germany

[5] Heraeus Precious Metals GmbH & Co. KG, Heraeusstr. 12-14, 63450 Hanau, Germany

* Correspondence: thomas.leissner@mvtat.tu-freiberg.de

Abstract: The recycling of proton exchange membrane water electrolyzer (PEMWE) raw materials is imperative due to their scarcity, cost, complexity, and environmental impact. This is particularly true in the context of expanding electrolyzer manufacturing and reducing production costs. Developing comprehensive recycling strategies requires the creation of a model stack due to the diversity in stack design, structure, and material. The review derived model presented here provides a sound basis and summarizes the variety found in literature and industry. The holistically developed recycling chain, including dismantling, mechanical processing, hydrometallurgical processes and carbon reuse, is characterized by the complete recycling of materials, the reduced application of energy-intensive process steps and the avoidance of environmentally harmful processes. Emphasis is placed on demonstrating non-destructive disassembly of joined components, dry mechanical decoating of catalyst coated membranes, membrane dissolution, separation of anode and cathode particles, and environmentally friendly hydrometallurgical processing of platinum.

Keywords: PEMWE; recycling; stack design; disassembly; mechanical processing; hydrometallurgy

1. Introduction

Green hydrogen is seen as an essential building block for sector coupling and paves the way for new decarbonization paths. Such sectors where CO_2 generation is difficult to abate include, for example, refining, aviation, shipping, and road transport, iron and steel production, cement industry, chemical industry and high-temperature industrial heat [1]. Green hydrogen is considered inevitable in those sectors. To produce large quantities of green hydrogen required for the decarbonization of these sectors, the technology of water electrolysis must be scaled up. Water electrolysis is considered as the central and so far the most promising technology for clean, CO_2-neutral i.e., green hydrogen production [2]. As an important water electrolysis technology, proton exchange membrane (PEM) electrolysis is expected to grow strongly in the market due to its good load change behavior and possible operation in the partial load range. Compared to other technologies, it can respond more quickly to fluctuating electricity supply, e.g., from renewable sources.

As the installation capacity of electrolyzers increases, the recovery and recycling of critical raw materials used in PEM water electrolyzers (PEMWE) like iridium or platinum will also become more

important in the future. The criticality of the raw materials themselves [3], resulting from the security of supply and resource situation, and a sustainability claim associated with hydrogen technology are motivation for the development of an adapted circular economy for PEMWE stacks.

As no standard PEMWE stack design has been established in industry and research yet, a huge variably of technological designs are available [4–9]. Due to this high diversity, the development of suitable recycling approaches becomes more challenging as an adequate recycling concept must be tailored. Currently, the limited number of circular economy strategies for PEMWE stacks discussed so far focuses primarily on hydrometallurgical and pyrometallurgical recovery of the noble metals [10], any other materials are not in the focus.

A recycling approach, which combines automated disassembly and mechanical processing can increase the maturity of the recovered materials and enable further circular economy strategies such as reuse, repair or remanufacturing of selected components. These strategies are more environmentally friendly due to low energy consumption, avoiding fluorine emissions and the possibility to recover membrane and carbon materials. However, mechanical recycling approaches for PEMWE haven't been designed and introduced on a large scale so far.

In order to advance research on recycling processes, a PEMWE model stack defined to represent a potential scaled-up stack is described as a starting point for further investigations. For this purpose, the components are described individually based on the literature and evaluated with respect to recycling strategies. This is followed by a general overview of relevant recycling stages in different areas of the circular economy. Finally, the integrated mechanical and metallurgical process chain for the recycling of PEMWE is described and quantitative results for individual process steps are presented.

2. Model Stack of Proton Exchange Membrane Water Electrolyzer

The development of new or adopted recycling technologies needs a defined and representative material as a starting point. Due to the high diversity of PEMWE stacks [4–9], however, the representativity is not yet given, which is why a conceptual outline of a stack based on literature is worked out to illustrate the potential material flows in the recycling streams. For this purpose, the individual components first have to be examined with regard to their relevance for recycling. Then the various configurations are assessed in terms of their likelihood of use on the basis of component requirements and market penetration. To understand the individual components, first the stack structure and the principle of operation are described. A possible model stack is shown in Figure 1.
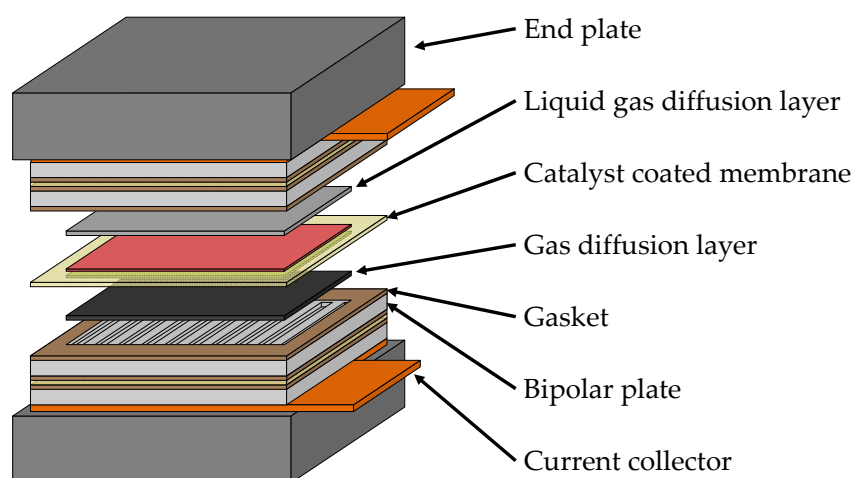
Figure 1. Model stack of PEMWE at the component level.

The electrochemical cell of the electrolyzer consists of a polymer electrolyte membrane (PEM - proton exchange membrane) and the electrodes applied to it. This composite structure is the core

element of the electrolyzer and is called a catalyst coated membrane (CCM) or membrane electrode assembly (MEA). This is where the electrochemical conversion of water to hydrogen and oxygen takes place, with hydrogen ions i.e., protons serving as charge carriers. On both sides of the CCM there are porous transport layers (PTL), which are also called gas diffusion layers (GDL) on the cathode side and liquid gas diffusion layers (LGDL) on the anode side. During operation water and the product gases flow through these layers. They also contribute to closing the electrical circuit. Bipolar plates (BPP), which ensure the inflow and outflow of reactants and products as well as the overall mechanical stability of the cell and close the circuit as current collectors, complete the repeating unit on both sides. Since the hydrogen production rate of one electrochemical cell is limited, multiple repeating units are combined into a stack to increase the overall power uptake and performance of the electrolyzer. The stack is framed by two massive end plates, which ensure proper sealing due to the uniform pressure distribution between layers in the repeating units. The compression derives from a tensioning system such as tie rods and screws. In order to apply electrical current to the stack, one current distributor plate is used at each end of the stack between the multiple repeating units and end plates [11]. In addition, gaskets inside the stack provide an additional sealing functionality and equilibrate tolerances that may occur during operation.

Looking at the scientific literature [4–9] and the commercially available stack components on the market [12–19], differences in the characteristics and properties of the respective components are evident. The large number of variants of PEMWE stacks is clearly illustrated in a so-called morphological box in Table 1. The individual components, their properties and different characteristics are described in detail below. The characteristics marked in bold in the morphological box are those commonly used.

2.1. Catalyst Coated Membrane

For recycling, the mechanical properties and the recyclable material content are of primary importance, as they have a major influence on the recycling approach. Since the critical raw materials, such as precious metals, are mainly contained in the electrodes, which form the special composite structure of the catalyst coated membrane (CCM), this component is considered first. In addition to CCM, there are other types of MEA designs, such as porous transport electrodes (PTE), where the catalyst is applied directly to the porous transport layers. Since the production and structure of CCM differs from that of PTE [20], a different recycling approach is required for the latter. For this reason, and because CCM is used almost exclusively, PTE is not considered further in this study.

2.1.1. Anode

The layered material composite must meet the highest requirements for mechanical and chemical stability and for electrochemical functionality. For this purpose, highly stable and electrochemical active materials are used to withstand the harsh operating conditions. On the anode side in particular, the high electrode potentials and the oxygen generated lead to corrosive conditions, which means that only certain precious metals can be used as catalyst. Because of suitable catalytic activity and high corrosion resistance, iridium is mainly used in pure as iridium black, mixed-metal or oxide form for oxygen evolution reaction [5,21]. Ruthenium, by contrast, has better catalytic properties, but is not stable enough in the long term under the conditions mentioned above [22]. Since iridium has very low market availability and is much more costly, mixed oxides of iridium and ruthenium are also used, which are a compromise between stability, activity and price [22]. The use of irdium-ruthenium oxide mixture reduces material availability problems for large-scale production.

Table 1. Morphological box of PEMWE stack components and their different characteristic variants derived from literature.

Components	Different. Properties	PEMWE Manifestations								
Membrane & Catalyst layer	membrane material	Perfluorosulfonic Acid (PFSA)			Hydrocarbon					...
	membrane thickness	51 µm	←→	127 µm	←→	254 µm				...
	anode material	IrO_2		Ir black		$IrRuO2$		Ir mixed metal		...
	anode loading	...	0.3 mg_{Ir} cm^{-2}	←→	1 mg_{Ir} cm^{-2}	←→	3 mg_{Ir} cm^{-2}			...
	anode layer thickness	...	2 µm		←→		12 µm			...
	cathode material	Pt black		Pt carbon supported		Pd				...
	cathode loading	...	0.1 mg_{Pt} cm^{-2}	←→	0.5 mg_{Pt} cm^{-2}	←→	1 mg_{Pt} cm^{-2}			...
	cathode layer thickness	...	8 µm		←→		21 µm			...
Porous Transport Layer	LGDL material	Ti								...
	LGDL thickness	...	100 µm	←→	250 µm	←→	2.000 µm	←→	3.175 µm	...
	LGDL specification	mesh		felt		foam		grid	sintered Ti-powder	...
	LGDL porosity	...	30%		←→		50%			...
	LGDL coating material	Au		Pt		Ir		...	none	
	GDL material	carbon								...
	GDL thickness	...	110 µm		←→		370 µm			...
	GDL specification	felt		paper		nonwovens				...
	GDL porosity	...	75%		←→		80%			...
Membrane electrode assembly configurations	Frame/Subgasket structure	yes						no		
		One-sided around CCM			Two-sided around CCM					
		GDL enclosed			GDL overlaid					
	Frame/Subgasket material	PI	PEN	PEEK	PPS	PTFE	...			
Bipolar Plates	bipolar plates material	Ti		stainless steel		graphite		Al		...
	bipolar plates coating	yes				no				
	bipolar plates coating material	Pt	Au	Ti	Ir	Nb	...			
	bipolar plates thickness	...	300 µm		←→		3.000 µm			...
	flow field	integrated flow field			flow field as separate component					
Sealing Elements	material	PTFE	silicone	Teflon	FKM	EPDM	PVD	PFA	rubber	...
	thickness	...	250 µm		←→		1.640 µm			...
	production/ joining method	injection moulding		screen printing		dispensing				...
	sealing concept	sealing on MEA			sealing on bipolar plate					

Clamping System	end plate material	Al			stainless steel			…
	fixation/ compression elements	tie rod			tension bands			
	position of compression elements	inside			outside			
Stack layout & active area	stack format	rectangular / quadratic			circular			
	size stack area	…	0,0025 m²	←→	0,7 m²	←→	1 m²	…

Another way avoiding material scarcity and high production costs of PEMWE is to reduce the iridium content in the anode, which is one main current focus in electrode development [23,24]. The iridium loading can thus be reduced from 1-3 mg_{Ir} cm^{-2}, which describes the state of the art, to, e.g., 0.3 mg_{Ir} cm^{-2} without causing performance losses [25]. Also, an ultra-low iridium loading of, for example, 0.08 mg_{Ir} cm^{-2} is in the focus of research [26]. These low loadings are made possible either by very thin electrode layers or by carrier materials such as titanium oxide [27]. Nevertheless, in industry and most of literature state-of-the-art the anode is made of non-supported iridium oxide with a loading of 1-3 mg cm^{-2} [28]. Hence, recycling strategies should firstly be adapted to this reference iridium content.

The catalyst material discussed so far has a typical particle size of approximately 2 nm and it is embedded in a binder/carrier system [26]. Since the binder, composed of the same ionomers as the proton exchange membrane, is an electrical insulator but contributes to the mechanical stability and the dimensionally stable structure, the ionomer content should be optimized to maintain all the functionalities, but priorizing uniform current distribution in the anode, which is essential for the electrochemical reaction. A content of 5 to 33 wt% ionomer are commonly discussed in the literature [4,6,29,30]. For a low iridium loading on the anode side Su, Linkov and Bladergroen [29] reported an optimal ionomer content of 5 wt%, while Xu and Scott [31] described an optimal content of 25 wt%.

The thickness of the anode layer strongly depends on the iridium loading, the ionomer content and catalyst support. In the literature, the thickness varies between 2 and 12 μm [7,9,25,26,30,32], with Bernt, et al. [33] describing the best cell performance for a thickness of 4 to 8 μm, equivalent to 1-2 mg_{Ir} cm^{-2}. A thickness of 3 to 4 μm has been reported for lower loading of 0.34 mg_{Ir} cm^{-2} by Padgett, et al. [34].

For these aforementioned parameters it is not possible to define exact values due to the high geometrical diversity, so recycling strategies have to address these types of variations. Given that iridium is one of the most valuable materials utilized in PEMWE [3], the objective is to ensure its complete recovery without any losses. This encompasses the separation of the electrode from the membrane, followed by the subsequent metallurgical processing steps.

2.1.2. Cathode

The cathode layer, which is deposited on the opposite side of the proton exchange membrane, has a very similar structure. Commercially available catalyst materials, such as platinum on a carbon support, can be used because this layer does not have to withstand the harsh conditions of the anode. In PEM fuel cells (PEMFC), carbon supported platinum has also been widely applied. In addition to platinum, palladium is also a suitable catalyst for the hydrogen evolution reaction [8]. Palladium is used as well as a carbon supported catalyst [7], which is currently in the focus of research [5]. However, palladium shows slightly lower electrochemical performance than platinum [35] and the cost advantages of palladium as previously described [5,36] are no longer applicable in the context of the current raw material prices (Q1/2025). Since 2019, the price of Pd has been significantly higher than that of Pt; by early 2024, raw material prices of platinum and palladium had converged [37].

The 8 to 21 μm thick layer [9,25,26,33] of the cathode consists of the catalyst, which is usually applied to a porous carbon support to minimize the platinum loading and to increase overall catalytic active area. Typically, a ratio of 40 to 60 ma.% metallic platinum is used as catalyst on industrial carbon black or on other carbon supports, such as carbon nanotubes (CNT). A very common support material is Vulcan XC72 from Cabot Corporation since it is also used a lot in PEMFC. Likewise, TEC10V50E from Tanaka Precious Metals Group Co., Japan [13] with a platinum ratio of approx. 46%, which was developed for PEMFC, is often applied as catalyst powder [6]. Since the platinum content, its particle size and local distribution within the CCM at the End of Life (EoL) are affected by degradation and dispersion phenomena [26], the initial ratio of platinum to carbon it is not relevant for the selection of recycling strategies.

Starting from the raw material, the platinum loading amounts to 0.5-1.0 mg_{Pt} cm^{-2} [4,5], which can already be reduced to 0.1-0.3 mg_{Pt} cm^{-2} in current research [26,38,39]. Analogous to the anode, a binder with mass fractions of 20-30% [4,30] is again used to ensure stability and proton transport.

As the recycling of platinum and/or palladium catalysts represents the current state of the art in PEMFC recycling [40], the metallurgical recovery of these precious metals from the cathode will not present a significant challenge. In addition to the goal of recycling the cathode without dissolving the precious metals, i.e., directly recycling the components, the objective is to identify a more environmentally sustainable approach that does not require the use of highly corrosive chemicals. In the context of mechanical recycling, the layer structure represents the most significant factor.

2.1.3. Membrane

The namegiving core element of a PEMWE is the proton exchange membrane also called polymer electrolyte membrane. It fulfills the functions of a reactant barrier to avoid gas permeation, electrical insulator between the electrodes to avoid a short circuit and proton conductor to close the electric circuit via charge carriers. In addition, it provides a mechanical stability for the electrodes, which are commonly applied to the membrane. Considering the harsh electrochemical operating conditions, the material also has to demonstrate a low gas permeability at high pressures and an excellent chemical stability [4,7,41].

Based on these requirements, only certain materials are eligible for proton exchange membrane whereby perfluorosulfonic acid (PFSA) is the most outstanding. Looking at the structure of the polymer, the polytetrafluoroethylene (PTFE) backbone provides a high mechanical, thermal and chemical robustness whereas the high proton conductivity is triggered by the perfluorinated side chains in the polymer ending with a hydrophilic sulfonic acid group [42]. Initially, PFSA was used because it is also applied in PEMFC and was readily available with various membrane thicknesses of 51 to 254 µm, depending on the supplier [18]. Thereupon it has established as electrolyzer material despite some serious disadvantages.

On the one hand, high costs in production and in disposal originate from the fluorochemistry applied here. In case of pyrometallurgical treatment for the recovery of platinum group metals, it is particularly important to neutralize evolved toxic gases, e.g., hydrogen fluoride [43]. On the other hand, at temperatures above 80°C the membrane looses the mechanical integrity and emits water leading to a decrease of ionic conductivity [43]. This temperature dependency restricts the window of operation of the PEMWE. Furthermore, the membrane becomes permeable for gas especially at increased temperatures and high pressures leading to specific safety risks due to explosive gas mixtures of hydrogen and oxygen. In order to avoid this, thick membranes are utilized resulting in high resistance to proton transport [44] and an increase of ohmic losses [30,45]. PFSA membranes exhibit hygroscopic behavior, expanding and contracting with humidity and temperature fluctuations [46].

The best-known brand name for a PFSA membrane is Nafion® from Chemours (formerly DuPont). It was widely used in PEMFC and has also established its use in electrolyzers [43,47]. Besides long-side-chain (LSC) PFSA, like Nafion®, Aciplex® and Fumion®, there are also short-side-chain (SSC) PFSA differing in essential properties. Aquivion® developed by Solvay Solexis is the best-known SSC-PFSA which can provide improved thermal stability resulting of higher degree of crystallinity and higher thermal transition temperatures [48]. In addition to PFSA-only membranes, there are composite membranes that are mechanically reinforced with another polymer such as PEEK (polyether ether ketone) or PTFE. Fumatech offers reinforced and non-reinforced membranes made of LSC- and SSC-PFSA in thicknesses of 60 to 150 µm [17]. GORE also offers an ePTFE-reinforced PEM with a thickness of 80 µm [15], which promises low gas permeability, a wide operating range and a more compact electrolyzer due to its reduced thickness.

Apart from PFSA, hydrocarbon membranes, i.e., sulfonated poly(ether ether ketone) and sulfonated polybenzimidazole, have also been the subject of research for some time as these have low production costs and, even more importantly, do not require fluorine chemistry [43]. Some

investigations were also carried out for PEMFC, but they could not compete against Nafion® in particular due to the short lifetime [42]. As well for PEMWE, the hydrocarbon membranes show advantageous behavior, such as low gas crossover despite operation at high pressures and good thermal stability [43].

Since the membrane is the core of the MEA and provides mechanical stability, it is also of great interest for recycling. Due to the variety of membranes and the differences in mechanical properties, one recycling strategy will probably not fit all types. Thus, it is important to focus on the most commonly used materials and develop the strategy on that. Nafion® is predominantly used both in research and on the market, mostly limited to Nafion® N115 and N117 [8,32,45] with thicknesses of 127 and 178 μm. Over the past two decades, the trend in fuel cells has been towards thinner membranes [47]. It can be reasonably assumed that this development will also be seen in the further for electrolyzers. CCM manufacturers and some of the literature [43] refer to N115 as the state of the art, therefore, this paper also uses this type as the model membrane.

Since PFSA in CCM releases toxic fluorine gases during metallurgical processing [40,43], it is important for environmental reasons to separate as much membrane material as possible from the electrodes before these are submitted to a metallurgical process step. It is also worthwhile to recover PFSA as a product because of its material value [10,21,49], and researchers are ambitiously developing ways to reuse recycled PFSA in CCM through a recasting process [50,51]. To achieve this, the purest possible PFSA product must be obtained by mechanical methods or by dissolving the membrane.

2.2. Porous Transport Layer

The next functional layer in the electrolyzer is the porous transport layer (PTL), which is applied to the CCM from both sides, i.e., covering both the anode and the cathode side of the CCM. Important properties of the PTL are the electrical conductivity for contacting between the electrode layer and the bipolar plate and the corrosion resistance, especially on the anode side. In addition, this layer is responsible for the reactant transport and the mechanical support of the CCM [52,53].

The PTL at the anode side is a liquid gas diffusion layer (LGDL), since oxygen has to be transported as a product in addition to water as the reactant. The harsh conditions on the anode side again require highly stable materials [54], so titanium is commonly used in various variations. In research, sintered materials made of powder or fibers are mainly used [38,52,55], since small cell areas are involved [41]. For larger areas, titanium is more commonly used in the form of expanded metal [56], meshes [5,57], felts [38,57], foams [7,54,57] or grids [52]. For long-term stability, the layer can also be coated with iridium [7,38], platinum [7,49] or gold [53,58]. According to the literature, the thicknesses are usually between 250 and 500 μm, although thicknesses of up to 2 mm are have been reported [4,28,38,53]. Manufacturers like Bekaert offers LGDL in thicknesses from 100 μm to 2 mm [59], Mott Corporation offers LGDL in 254 to 3175 μm thickness [14] and GKN Powder Metallurgy GmbH offers among others type T3P in a thickness of 1300 μm [60]. Porosity between 30 and 50% is considered optimal [55,61,62]. If this layer does not adhere to the CCM, no further mechanical processing will be required as the LGDL can be separated already by destacking. Thus in this case, the LGDL could be sorted for further recycling or reuse. If the LGDL sticks to the CCM due to clamping pressure, the titanium component should be removed from the CCM. During this process, parts of the electrode may adhere to the titanium, which should be removed by cleaning to avoid losses and achieve the high recycling rate.

On the cathode side the gas diffusion layer (GDL) is made of carbon since there are no special requirements for the material durability and stability except for hydrogen embrittlement for some metals [4]. Similar to GDL in PEMFC carbon felt, paper and nonwovens are used [10,49]. Predominantly carbon fiber papers of the trademark Toray® are applied with thicknesses between 110 and 370 μm and porosities of 75 to 80%, mostly 78% are stated [12,63]. Other manufacturer are SGL Carbon SE [19] or Freudenberg SE [16] offering GDL with thicknesses of 150 to 315 μm. GDL with a microporous layer (MPL) for reduced electrical resistance and improved mass transport can

also be implemented [41,54]. As the GDL is usually bound together with CCM in the seal and adheres to the CCM due to the clamping pressure, further challenges arise during mechanical processing, such as the liberation and subsequent sorting of the shredded product. If the fibers of the GDL can be obtained by mechanical and hydrometallurgical processes, they can be reused at the end of the process chain, for example in carbon-bonded alumina [64].

2.3. Membrane Electrode Assembly Configurations

In the context of the PEMFC, there is no uniform definition of the structure or design of the MEA. Ma at al. 2022 described a three-layer MEA consisting of membrane and two catalyst layer (CCM). In a five-layer MEA, the CCM is framed within subgasket layers. A seven-layer MEA consists of both-sided subgasketed CCM with anode and cathode-side GDL [46]. Synonyms for subgasket are frame or edge protection. It provides sufficient robustness and mechanical durability to the MEA. Considering sufficient insulation between anode and cathode, typically malleable plastics such as PI (polyimide) or PTFE are used [20,65]. The provider CMC Klebetechnik GmbH [66] also offers PEN (polyethylene naphthalate), PEEK and PPS (polyphenylene sulfide) subgasket films for PEMFC and PEMWE.

These various MEA configurations are also known for PEMWE. Bernt, Schröter, Möckl and Gasteiger [6] showed a MEA structure with a single-sided subgasket on the anode side [6]. Mayyas, et al. [67] described a structure in which the CCM is enclosed by a frame on both sides at the edge areas. In a study from Stähler, Stähler, Scheepers, Lehnert and Carmo [65] a 12 μm thick subgasket was used to protect the thin membrane from the sharp edges of the titanium PTL. Holzapfel, Bühler, Van Pham, Hegge, Böhm, McLaughlin, Breitwieser and Thiele [20] also specifies a MEA structure with two-sided frame. When using a subgasket, there are several different assemblies. Either the CCM is encased in the subgasket and the GDL is then attached to the subgasket. Alternatively, the subgasket can encapsulate both the CCM and the mounted GDL. Subgasket films are typically supplied with adhesive on one side and joined by laminating under pressure and/or heat [66]. Without the use of a subgasket, the seal is located directly between the bipolar plate and the CCM.

The variety of MEA configurations with subgaskets presents a challenge in determining the appropriate process for MEA recycling. In the most straightforward scenario, the absence of a subgasket renders the recycling process unaffected. However, in instances where a subgasket is present, its removal or shredding and sorting is necessary to facilitate the recycling of the remaining MEA components.

2.4. Bipolar Plates

The functions of the BPP in the PEMWE stack are to ensure media transport, electrically contact the PLT, transfer heat, and provide mechanical stability. Currently BPP are typically made of titanium. Lower cost materials such as stainless steel e.g., AISI 304 or 316L could significantly reduce the overall system cost of an electrolyzer system [68]. Stainless steels are cheaper and easier to machine than titanium, but the main drawback is their corrosion at high chemical overpotential within an oxidative medium [4,8,69]. For this reason, a bipolar plate made of stainless steel must be protected with a highly conductive and corrosion-resistant coating. Highly conductive and corrosion-resistant coatings made of titanium, platinum, niobium, niobium/titanium, gold or iridium can further protect against the corrosive environment [5,7,67,69,70]. Other BPP materials mentioned in literature are graphite and aluminium [7].

According to Bareiß, de la Rua, Möckl and Hamacher [9], PEMWE BPP consists of thicker materials than PEMFC BPP due to the higher operating pressure. They are between 0.3 mm and 3 mm thick [9,71] and can be produced using various manufacturing processes such as sheet metal forming, destructive milling or plate etching [9]. As stated in a patent, the stack manufacturer Hoeller Electrolyzer GmbH produces bipolar plates by sintering [72].

Regarding the flow field in the bipolar plates, the parallel channel configuration remains the most common design in PEMWE. The flow field design has to ensure the uniformity of the fluid flow

and pressure distribution to enable high pressure operation and high current density in the stack. The flow channels are machined or stamped directly on the BPP surface [73]. In addition to this cell design with BPP with integrated flowfield, Borgardt, et al. [74] describe further designs. Alternatively, the cells can also be designed with BPP without a flowfield. In this case, a titanium mesh acts as a PTL to transport the media [73,74], which has implications for disassembly and handling of the components in recycling processes.

The objective of recycling BPP is to maintain the titanium within the material cycle. This can be achieved by incorporating the material into titanium recycling or by developing an effective reuse and remanufacturing process.

2.5. Sealing

Gaskets in PEM cells are used to seal the anode and cathode chambers and prevent gas crossover and the escape of water, hydrogen and oxygen. A further requirement for the gasket is to achieve optimum contact between the components. To fulfil the requirements for the operating conditions in PEMWE stacks, the gaskets must have appropriate mechanical and chemical properties [71]. According to the study by Borgardt, Giesenberg, Reska, Müller, Wippermann, Langemann, Lehnert and Stolten [74], the optimum clamping pressure for PEMWE stacks amounts to 2.0-3.0 MPa [74]. Gasket materials used to fulfil the requirements are usually FKM, EPDM, silicone and PTFE [6,49,71,75]. Suppliers of PEMWE gaskets include the companies Freudenberg Sealing Technologies or Chemours. Usual material thicknesses amount to between 250 and 1640 μm and depend on the gasket material, the stack design and the operating pressure in the stack [49,71,76]. The gaskets are either directly applied to the BPP or the MEA by dispensing or screen printing or alternatively inserted between the BPP and MEA as an injection-moulded O-ring gasket.

Similarly, the situation with the subgasket of the MEA is analogous to that described above. The more firmly the seal is applied to the MEA, the more effort is required to remove it from the supporting components. This can result in the loss of valuable materials, such as adhering catalysts, and the contamination of the products.

2.6. Clamping System

The clamping system establishes the sealing pressure and the correct distribution of the clamping pressure between the various cell components, which reduces the contact resistance between the interfaces. A high clamping pressure increases the contact area between the BPP and the PTL, which reduces the electrical contact resistance between the elements. The clamping pressure therefore plays an important role in optimizing the performance of the stack [71]. Stiff end plates are used at the ends of the stack to maintain the clamping pressure. The materials used for end plates should provide high electrical insulation, high thermal conductivity, stability and rigidity as well as corrosion resistance. To fulfil these requirements, end plates are usually made of aluminium or stainless steel and are regularly several centimeters thick [7,76]. Unlike PEMFC, which use tension straps in addition to tie rods [67], PEMWE end plates are bolted together with tie rods for tensioning and compression. The tie rods, which consist of bolts and nuts and are tightened with washers or disc springs, can be located outside or inside the cell stack and guided through boreholes in the cell components. In order to minimize ohmic losses, the stacks must be pressed to an optimum force. Compression forces of around 2.5 MPa are mentioned in the literature for PEMWE stacks [71,74].

The specific design and structure of the clamping system and the end plates are of particular importance with regard to disassembly. In the context of subsequent material recycling, the material composition of the components is of significant importance, as this determines which recycling route can be taken.

2.7. Stack Layout

There are major differences between manufacturers in terms of stack format and size. In principle, a distinction is made between circular and rectangular stacks. According to a study by Smolinka, et al. [77], PEMWE stacks in production scale have a cell area of less than 1 m² (active area including edge). Further literature and a look at the stacks of various manufacturers such as Siemens Energy, Bosch, H-TEC, HIAT and HOELLER also reveal that the commercial stacks at the moment offer an area per cell of approximately between 0.0025 and 0.7 m² [78–80].

Commercial electrolysis systems such as Siemens Energy's have a power input of 17.5 MW with hydrogen production of up to 2000 kg per hour. The system has a modular design and consists of 24 identical and connected electrolysis stacks [81]. Hoeller Electrolyzer GmbH offers three different stack sizes with stack power inputs from 76 kW to 1.4 MW (hydrogen production 34 to 635kg per day per stack) [82]. With dimensions of 85 cm x 100 cm x 153 cm and a power input of 1.25 MW, the Bosch electrolysis stack is designed to produce up to 23 kg of hydrogen per hour [83].

3. Recycling Process

3.1. General Recycling Approaches

After describing the electrolyzer and its components in detail and identifying the components relevant for recycling, the recycling processes in general are outlined below.

Before an item can be recycled, it must be assessed according to the EU Waste Directive of 2008 [84]. This directive defines a five-level waste hierarchy, which begins with preventing an item from becoming waste, for example by extending its life time or reusing it. The next level is preparing for reuse, which involves testing, cleaning, and repair. In the case of an electrolyzer, certain components such as the bipolar plates can be removed from the stack, and there are realistic options for their reuse after refurbishment or remanufacturing. Recycling of waste is the next level in the hierarchy and aims to use appropriate processes to reprocess waste into products, materials, or substances that can be used for their original purpose or for other purposes. It is important to recover as much material as possible and maintain material quality as far as possible.

To facilitate reuse and recycling, manufacturers should develop a disassembly-friendly design [85]. Before considering waste disposal methods such as landfilling or incineration, efforts should be made to recycle the waste in other ways. Options for recycling include using it as a fuel or other means of generating (thermal) energy [84].

As soon as an object is destined for recycling to recover valuable materials, it passes through the four steps of the recycling chain according to Martens and Goldmann [86], depending on the type of waste. The general recycling chain includes following steps:

1. Collection and pre-sorting
2. Pretreatment and disassembly
3. Mechanical and chemical processing
4. Production of secondary (raw) materials

These steps have to be adapted to the product to be recycled. Kumar [87] suggests a similar term for the processing of e-waste without naming the collection, pre-sorting and pretreatment. For lithium-ion batteries (LIB), Werner [88] explained the general steps of the recycling chain in his paper as follows.

5. Preparation: waste logistics and presorting
6. Pretreatment: dismantling and depollution
7. Processing: liberation and separation
8. Metallurgy: extraction and recovery

Since there are certain similarities between LIB and PEM technologies, e.g., demountable structure, metal-containing electrodes or layer structure of the entire system, it is reasonable to take a closer look at this recycling chain. Individual steps can then be adopted or adapted.

The first step, i.e., preparation, includes waste logistics and presorting, as described by Martens and Goldmann [86]. Transport, which is in the responsibility of business logistics, is also necessary for PEM technologies such as fuel cells and electrolyzers due to the intended quite decentralized use. Already in the logistics presorting can be organized according the fuel cell and hydrogen principle (alkaline, high temperature and PEM). Further presorting of different PEM technology types accounts for the different components or materials used in each.

For LIB, pretreatment consists of dismantling of battery systems and depollution. The latter, relates to chemical, electrical and thermal hazards. Depollution would not be necessary for PEMWE or FC since there is no residual charge or any volatile solvent within the EoL set-up. With PEM technologies, disassembly is possible down to the repeating unit or even down to the level of the individual components, such as the bipolar plate and MEA [40].

Since no general mechanical recycling route has been defined for PEM technologies yet, only individual steps as liberation and separation can be named for the processing, which currently is subject to research [89,90]. Nevertheless, these two steps can provide valuable feed materials for metallurgy. For LIB, the liberation step may also include thermal pretreatment to decompose the binder in the electrodes to facilitate the decoating of the support structure, the electrode foils respectively [91,92]. Since in PEM technologies the binder and the membrane are made of the same material, a thermal treatment is not an option to improve the liberation. The membrane would also decompose, releasing toxic gases. This approach requires a thermal metallurgy process without a mechanical process, and the membrane material can no longer be recycled in this way.

Metallurgical processes to produce secondary raw materials that can be returned to the material cycle are state of the art for PGM [7,21,89]. For platinum catalysts in particular, established processes can be adopted from the fuel cell industry. It is important to note that most PEMFC recycling has focused on platinum only and not at other valuable materials. This means that no mechanical processes can be transferred from the PEMFC to WE.

3.2. Process Chain for PEMWE Recycling and Proof of Principle Tests

The conceptual design of a possible process chain for the recycling of PEMWE has been developed, which contains some variants. The feed material is a model PEMWE stack as described in section 1.

First, the end plates, bipolar plates with seal, clamping elements and the MEA are demounted applying manual or automatic disassembly (see Figure 3). Either a higher dismantling depth is possible and the GDL and PTL can be demounted as a whole or the MEA has to be shredded into its GDL, PTL and CCM components. The next process sorts the liberated MEA components into their respective fractions. Since the CCM is a composite structure containing critical and valuable target elements, it has to be considered further and the CCM is cut into smaller, more manageable pieces that can then be fed into the decoating process.

Mechanical decoating, which removes the catalyst layers from the polymeric membrane, can be performed with an impact stress that liberates both electrode layers from the flexible polymer membrane. The decoating produces a precious metal containing electrode powder and a PFSA product of larger decoated membrane pieces (see Figure 4a).

Since the electrode powder contains both anode and cathode active materials, a mechanical separation process (see Figure 6) can be applied to the ultrafine particles to generate a concentrate for the subsequent hydrometallurgical processing. If a high grade and a sufficient yield cannot be reached with the mechanical separation methods, the entire electrode product can be leached as well. Leaching produces a platinum and an iridium containing solution that can be further hydrometallurgically processed. Leaching also produces a carbon product from the cathode-side catalyst supports and it can be processed into carbon-bonded materials in a reuse process.

A variant of mechanical decoating of CCM, dissolves the membrane in a suitable solvent followed by filtration and is alternative approach to separate the electrode material from the fluorinated membrane. The filtration can become challenging, since the particles are below 10 µm

leading to a high filtration resistance, which leads to a high operation pressure drop. Furthermore, the increase in viscosity due to the dissolved ionomer also effects the pressure drop in the filtration step negatively. The PFSA material from the membrane is recovered as a clear ionomer solution. It may also be useful to dissolve the mechanically decoated membrane pieces, as there may still be electrode residues on or precious metal particles within the membrane due to aging effects. Figure 2 shows a flowchart of the mechanical and hydrometallurgical recycling chain, followed by a more detailed explanation of some of the process steps in the chain and quantitative research results.

3.2.1. Disassembly into Individual Stack Components

The material-specific separation of products by disassembly has the potential to significantly increase the recycling yield and the grade for precious and critical metals. Due to its preconcentration, it simplifies the mechanical and metallurgical processing downstream. The repair and reuse of products and the harvesting of components for reuse all require simplified access to product components and its joints. Disassembly thus enables the implementation of these further circular economy strategies [93] and it is of great importance that the disassembly is set up in a non-destructive procedure.
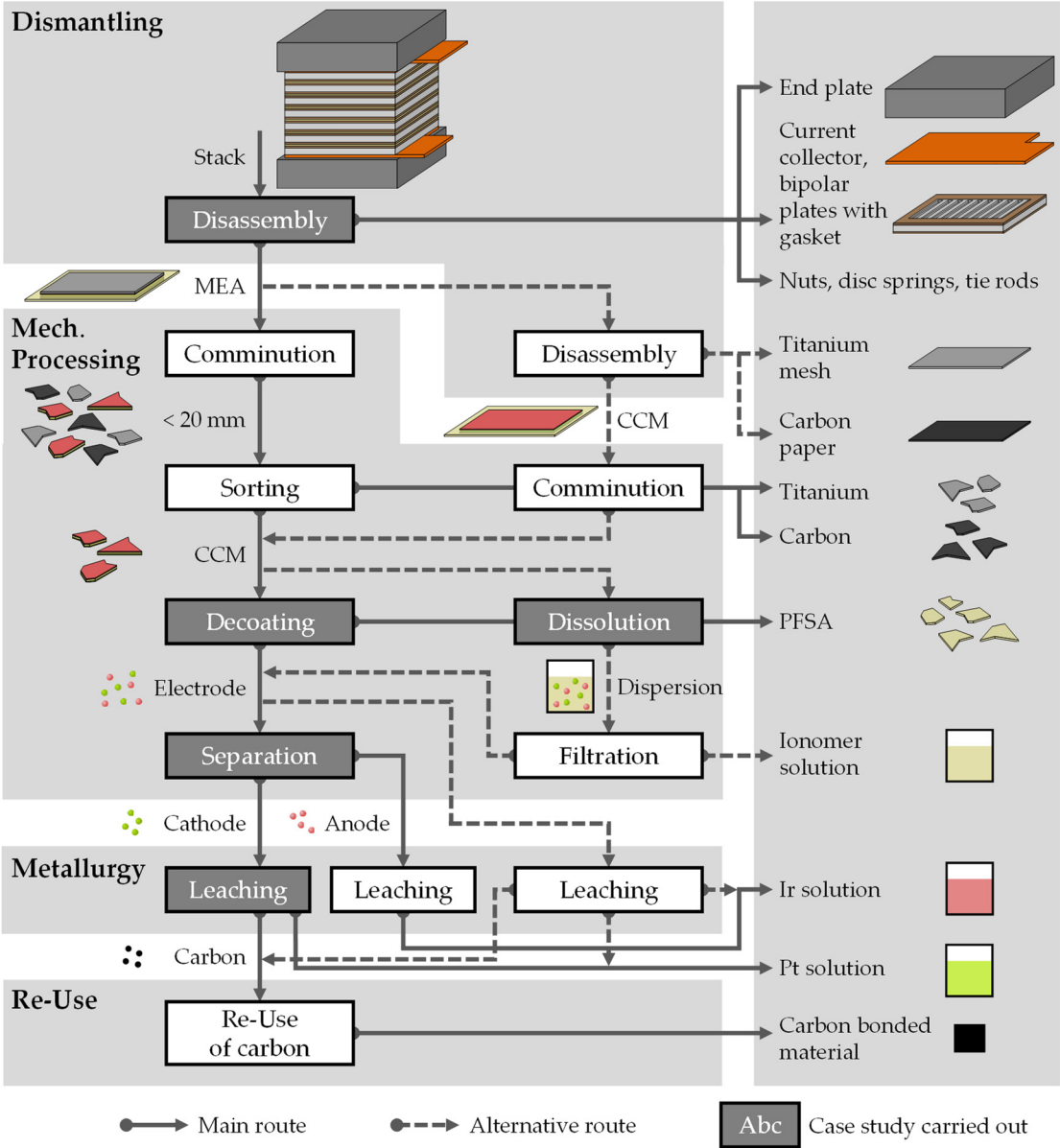
Figure 2. Conceptual outline of a combined mechanical and hydrometallurgical recycling chain for PEMWE; colored process steps have been investigated experimentally (proof of principle trials).

In Al Assadi, Goes, Baazouzi, Staudacher, Malczyk, Kraus, Nägele, Huber, Fleischer, Peuker and Birke [85], the challenges of disassembling PEMFC have already been highlighted. As fuel cell stacks and electrolysis stacks are comparable in terms of macroscopic product structure, the challenges mentioned can be transferred. A major challenge for disassembly is the adhesion of the stacked layers to each other, which originates from the compression, operation, and aging itself and not primarily from the manufacturing process. It predominantly occurs in the sealing area between the stacked layers. Furthermore, the accessibility of this joint is also constrained by the layered structure, the small component pitches and the low material thicknesses.

The two main components MEA and BPP exhibit different degradation mechanisms. Typical degradations of the catalyst layer and the membrane are dissolution, poisoning, sintering, and catalysts passivation. Degradation of the bipolar plates leads to embrittlement and corrosion [94]. A typical cause of stack failure is perforation of the MEA [95]. The MEA or the membrane is therefore in general the component that limits the lifetime of the stack [9,95,96], while the BPP can have a significantly longer durability.

Mayyas, Ruth, Pivovar, Bender and Wipke [67] provide an overview of the manufacturing cost structure of PEMWE stacks. The largest share of the costs of the CCM or MEA is attributable to material costs such as membrane and PGM costs. In contrast, the material costs for substrate material and coatings or bipolar plates are low and the production costs predominate here.

Circular Economy strategies can be derived from the duality between MEA and BPP in terms of degradation and cost structure: Given that the MEA is the component that limits the lifetime and has a high material value, this component is forwarded for recycling. In order to maintain the high value-added share of the BPP, repair or remanufacturing should be realized before recycling [97]. This results in requirements for the disassembly process: non-destructive and sorted disassembly and separation of the components of the PEMWE stack. In the scenario of a repair, it must be possible to separate the stack at any point within the layered construction.

As the bonding of the components in an EoL stack can be compared to an adhesive bond, DIN/TS 54405 should be used to derive a suitable separation process [85,98]. This divides the processes into mechanical, physical and chemical methods. Only the mechanical methods of cutting and peeling and also shearing can fulfill the requirements for a non-destructive process, if it is applied to the joint, the sealing area respectively. Physical and chemical processes such as cooling and heating can be used as aids to render the sealing gasket brittle or to exceed its glass transition temperature and thus reduce the strength and the adhesive force. The use of solvents or blowing fluids can also weaken the adhesion points. The accessibility within the stack structure is also a limiting factor here and a certain reaction time of the solvent must be considered, which would extend the disassembly process time. The solvent can also make subsequent reprocessing of the bipolar plates more difficult and generates additional challenges in work and environmental protection.

A mechanical separation process to demonstrate non-destructive disassembly using a cutting tool and the corresponding equipment is presented in Figure 3. The process has been validated for fuel cell stacks and could be transferred to electrolysis stacks. The equipment includes a lifting table on which the stack can be adjusted in height. Two linear axes, on which a cutting tool is mounted, can be adjusted synchronously or asynchronously and can guide a wedge through the stack. A robot is used to manipulate the separated components. Using the process described, a non-destructive disassembly can be realized.
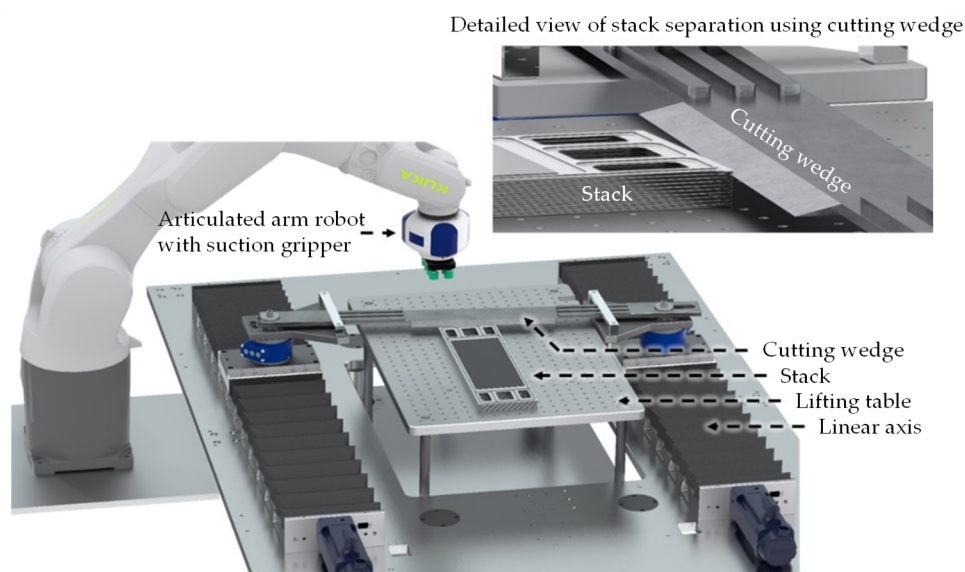
Figure 3. Equipment for disassembling a stack into its individual components using a cutting tool.

3.2.2. Decoating of Catalyst Coated Membrane

After disassembly of the end plates and separating the BBP from the MEA the subsequent step is the decoating of the electrode from the membrane. As it is not clear how the PTL and GDL can be removed, the mechanical decoating is focusing on the CCM.

The advantage of mechanically decoating of the CCM is that the fluorine-containing membrane is liberated from the valuable electrode materials without the use of solvents or the emission of harmful hydrogen fluoride, which reduces the environmental impact. The membrane material can be recovered as polymeric material, unlike hydro- or pyrometallurgy where the membrane is decomposed.

Since actually the installation of high electrolyzer capacity is still pending the availability of sample material is limited. Therefore, the experiments were scaled down and a micro-scale hammer mill was used on samples sizes of < 100 mg to investigate the separation and liberation of the electrodes by mechanical processes. The Picocrush hammer mill with a discharge screen belonging to the Hosokawa Alpine's Picoline machine platform is the only available comminution machine that can process CCM samples of several millimeters in size in very small quantities. With this machine, samples of less than 100 mg with a diameter of 5 mm can be processed at various speeds, i.e., various specific energy consumption. During this process, the electrode is liberated from the membrane by impact, while the membrane sample remains intact in most cases. It was necessary to develop quantitative analysis methods to meet the requirements set by the small masses and the properties of the samples. The elemental mapping of a μXRF analysis can be used to distinguish the remaining coating and the decoated areas of the CCM based on the dominant elements, which allows to quantify the decoating efficiency. For this purpose, iridium and platinum are used as indicators for the anode and cathode, respectively, while areas with a high sulfur content are assumed to be decoated, since the PFSA membrane is directly accessible here. An example of such a μXRF mapping is shown in Figure 4a, which illustrates the cathode side of a partially decoated sample.
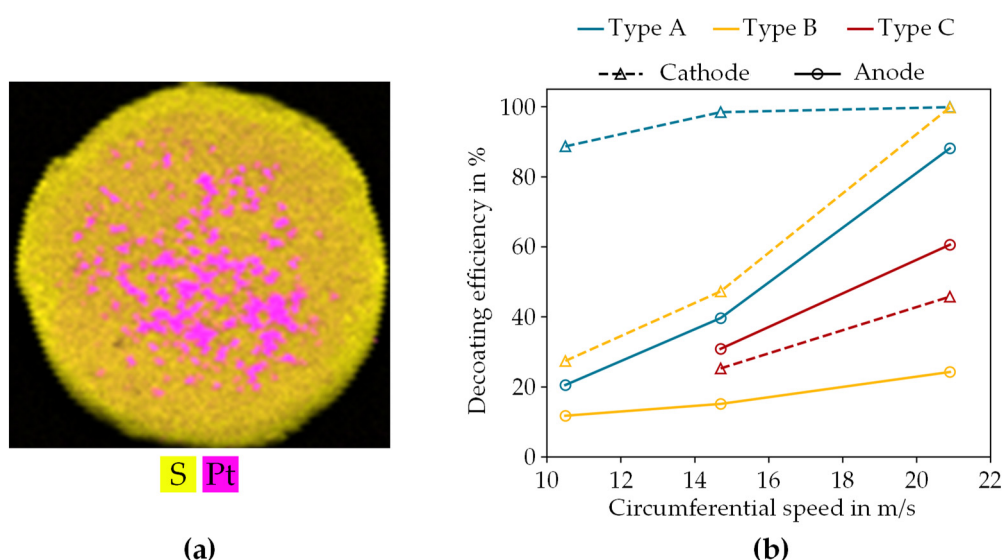
Figure 4. (a) µXRF mapping of sample indicating sulfur and platinum, cathode side of type A milled at 10,2 m/s with calculated decoating efficiency of 88,0%; (b) Decoating efficiency for three types of CCM in laboratory hammer mill as function of the circumferential speed (circular discharge screen size 1 mm).

The investigation results are summarized in Figure 4b for different types of CCM. It shows that with increasing speed, the anode and cathode of each type continue to decoat and complete decoating is possible. However, the decoating efficiency, which is the ratio of the decoated area to the total area of the sample, depends on the type of CCM. For instance, type A shows a selective removal of the cathode at lower milling speeds, while the anode is mainly removed at higher speeds. This selective grinding is also CCM type dependent. Possible reasons for this are differences in the surface structure of the coating layer, such as cracks in the electrode that facilitate decoating, or the thickness and adhesion of the electrode layer, which are influenced during the manufacture of the CCM and the binder content. The extent to which the adhesion of the electrodes to the membrane can be influenced prior to decoating remains to be determined in further investigations.

Since the recovery rate of the critical precious metals must be close to 100 % for this process step to become relevant, further investigations need to be carried out at higher stressing intensities, higher speeds respectively.

If it is not possible to completely decoat the CCM using dry mechanical methods, an alternative process has to be used. This can be either a wet mechanical decoating process, for which alcohol treatment has often been used in research to date [49,90], and it must be clarified whether this process can decoat all CCM in contrast to the dry method. Alternatively, complete dissolution of the membrane and ionomer-containing binder can be used.

3.2.3. Dissolution of Catalyst Coated Membrane

An alternative process step to the mechanical decoating of the membrane is the complete dissolution of both the membrane and ionomer-containing binder. The sulfonic acid functionalized fluoropolymers (ionomers) that enable the proton conductivity through the membrane and the catalyst layers can thus be recovered as a further target material for recycling. It is as well an economic relevant target material, since the membrane used in PEMWE have high costs. A known method for the dissolution of these ionomers is the dispersion in alcohol-water mixtures at higher temperatures under pressure [99]. The ionomer dispersion can then be separated from other components, mainly the catalysts, by filtration or centrifugation. In this work, these procedures were successfully applied to different kinds of CCM. Some obtained precious metal yields are given in Table 2. Analytical methods to determine the ionomer content in the initial CCMs still have to be developed, an ionomer yield can therefore not yet be given.

Table 2. Precious metal yields of dissolved membrane after separation of ionomer dispersion.

CCM	Platinum recovery in residue (wt-%)	Iridium recovery in residue (wt-%)
Type #1 - Spent PEMWE	> 99 %	> 99 %
Type #2 - Spent PEMFC	> 99 %	Not contained

The examples show that within the precision of measurement a loss of platinum and iridium into the ionomer dispersion stream does not occur. In further steps of the downstream processing, the PGM-containing catalyst residue can then be processed by conventional pyro- and hydrometallurgical methods in order to recover the PGMs.

For the ionomer dispersion, definitely further work is necessary in order to evaluate further uses and decide on (direct) recycling or (chemical) down-grading. Knowledge about the chemical integrity of the polymeric ionomers and the impurity profiles is mandatory for this evaluation.

3.2.4. Separation of Anode and Cathode Materials

When the electrode and membrane are separated by one of the aforementioned processes, a mixture of the iridium-containing anode and the platinum-containing cathode is generated. Individual fractions of the two electrode types can be produced for efficient hydrometallurgical processing using mechanical separation processes.

Compared to mechanical separation, chemical methods consume more energy and require an overall higher processing effort. Thus, mechanical processes, which still require fundamental research, may provide an innovative and sustainable technological option to separate ultrafine particles below 10 μm [100–102]. Consequently, the development of physical separation processes for PEMWE recycling should be addressed.

As aforementioned, state of the art materials of two different electrodes are metal oxides of iridium or ruthenium and platinum on the support material of carbon black. Ahn and Rudolph [103] stated that the catalyst materials used in each electrode of the PEMWE show significant differences in their (de)wetting behavior. The hydrophilic and hydrophobic properties of TiO_2 and carbon black, which can be seen as the representative materials of anode and cathode active materials, reproduce this behavior. The static water contact angle of four different CCM samples was determined with the sessile drop method to confirm the result of the hydrophobic cathode surface in contrast to the hydrophilic anode in Figure 5. Although the degree of hydrophobicity varies by CCM type, the results are consistent with their work. As described in the discussion of decoating processes, this can also be an effect of the manufacturing process of the CCM or different binder content.
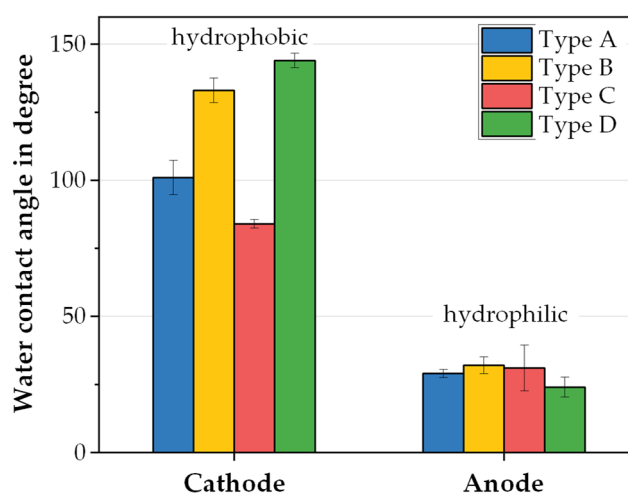
Figure 5. Water contact angle of anode and cathode side of different CCM types determined with static sessile drop method.

To utilize the different wetting properties of TiO_2 and carbon black, different methods such as froth flotation or liquid-liquid phase/particle separation (LLPS) can be applied to separate the two representative materials. Froth flotation is the most established separation process exploiting the different wettability of the particles as main separation feature. However, the separation of particles below 10 μm by flotation is challenging due to the low probability of particle-bubble attachment [104] as well as the entrainment of hydrophilic particles. In the previous study [105], the recovery and grade of the representative catalyst particles were achieved at 70 % and 90 % through froth flotation. This suggests the need for further improvements. LLPS is presented to overcome the limitation of this conventional separation method [106]. Two immiscible liquid phase systems allow the transfer of hydrophobic particles to the organic phase while hydrophilic particles remain in the aqueous suspension [107]. Based on the LLPS, using a model particle mixture of TiO_2 and carbon black, controlling the pH of the initial suspension and the adding of dispersant, allowed the recovery of each material of 97 % and 99 % with a grade of 97 % and 99 % respectively. TiO_2 ends up in the aqueous and carbon black in the organic phase as shown in Figure 6.
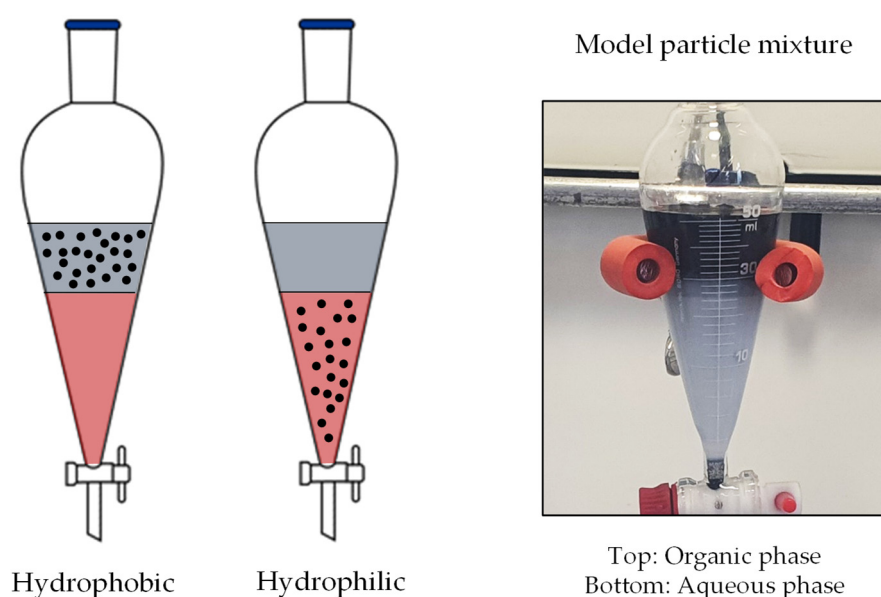

Figure 6. Scheme of LLPS for ultrafine particle separation. Hydrophobic particles stabilized in the organic phase and recovery of hydrophilic particles can be accomplished in the aqueous phase.

However, since amphiphilic ionomer is used as binder during the preparation of catalyst layers, ionomer adsorption on particles may occur, which affects the interaction between the particles and the phase of LLPS and become critical to the further design of the separation process. The alignment of ionomer molecules affects the surface properties of electrode powders, especially the wetting behavior of anode material changed to water repelling [108,109].

3.2.5. Leaching of Separated Platinum Catalyst from CCM Material
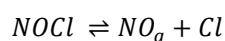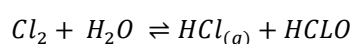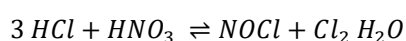
The next step downstream is the metallurgical processing of the concentrates from mechanical separation, often using a hydrometallurgical approach for the platinum-containing cathode. Precious metals can usually be easily dissolved using highly corrosive chemicals and chemical mixtures such as hydrochloric acid or aqua regia, which is also utilized as one of the primary leaching agents for platinum. Nevertheless, the use of aqua regia raises environmental concerns due to gas formation and its corrosive nature per se. To mitigate environmental concerns, alternative leaching solutions can be employed in the presence of chloride as a platinum complexing agent [110]. A more environmentally friendly platinum extraction process is being investigated here by using organic acids, such as acetic and citric acid with hydrochloric acid [111,112].

The small-scale laboratory leaching experiments were carried out as part of a preliminary study with synthetic material (platinum on carbon black purchased from Sigma-Aldrich (CAS: 7440-06-4)), which could be one concentrate originating from mechanical decoating and liquid-liquid separation in proposed recycling chain for PEMWE (section 3.2). The leaching results shown here intends to provide an initial orientation and assessment of the use of oxidizing agents and organic acids, that still need to be reproduced with further experiments. Varied leaching parameters such as temperature and leaching agents can be taken from Figure 7. Other leaching conditions such as solid-liquid ratio and stirring speed were kept constant throughout all experiments.
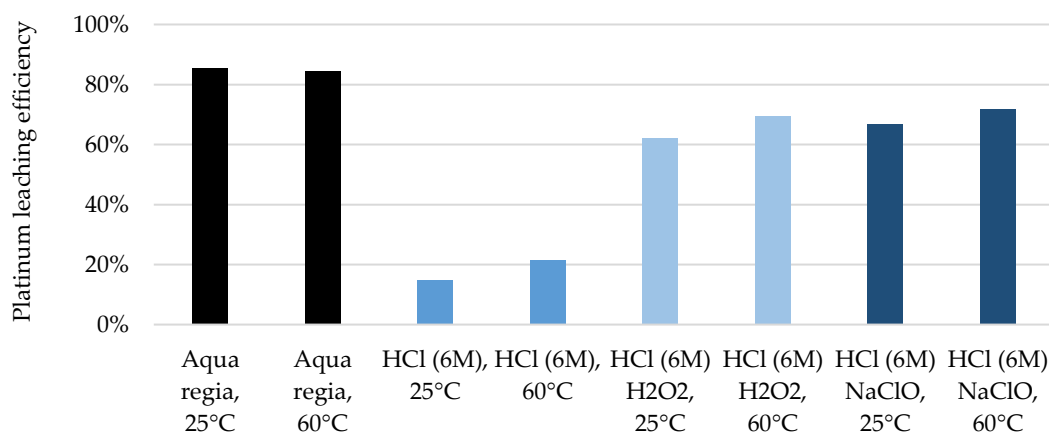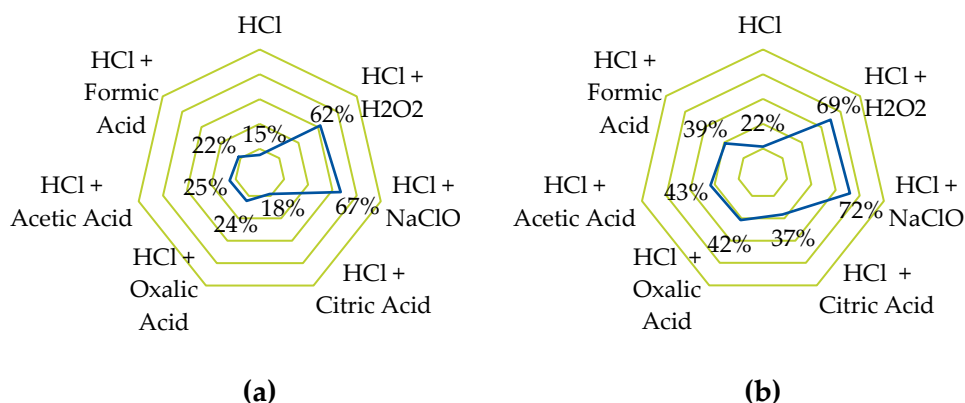

Figure 7. Leaching efficiency of platinum after 6 hours with aqua regia and with hydrochloric acid with and without oxidants (H_2O_2, NaClO) at 25 °C and 60 °C.

The platinum leaching with aqua regia has the highest efficiency, i.e., recovery in the leachate, amounting to > 80 % regardless of the temperature. The application and need of oxidizing agents have already been investigated [110]. The three main reactions from aqua regia are [113]:

$$3\ HCl + HNO_3 \rightleftharpoons NOCl + Cl_2\ H_2O$$

$$Cl_2 +\ H_2O \rightleftharpoons HCl_{(g)} + HCLO$$

$$NOCl \rightleftharpoons NO_g + Cl$$

It can be deduced from the reaction equations that Cl outgasses from the system over the reaction time as a result of the reactions. As HCl was not continuously added to the system in the experiments, the yield is lower than would be expected with aqua regia. The relevance of oxidizing agents during leaching of platinum can be seen in Figure 7. Sodium hypochlorite compared to hydrogen peroxide shows a slight additional increase in efficiency. Figure 8 illustrates the leaching efficiencies of platinum using organic acids in combination with hydrochloric acid.

Figure 8. Leaching efficiency, i.e., platinum recovery, after 6 h with hydrochloric acid with organic acids at 25 °C (a) and 60 °C (b).

The leaching efficiency of hydrochloric acid increases when it is combined with organic acids. Even if the efficiencies are still very low at around 40 % at 60 °C using organic acids, first tests using further oxidizing agents as well as salts show a high potential for leaching efficiencies of at least > 70 %. As higher efficiencies than 99 % are state of the art for platinum leaching, leaching efficiencies higher than 95 % should also be targeted for more environmentally friendly leaching agents, aiming in particular at sustainability and process intensification, but require further investigation and up-scaling.

After leaching, the liquid phase is separated from the insoluble carbon residue by filtration. The dissolved platinum can be recovered from the solution and the (re)use of the remaining carbon with residual platinum must be investigated. The optimization of the leaching and acid recycling will involve the optimization of the filtration and washing steps as well [114,115].

4. Conclusion

Due to the wide range of different PEMWE stack designs, it is challenging to focus on one single technological concept for recycling. Therefore, the whole variety in the literature was presented in a morphological box, and based on a literature review the relevant characteristics for a model stack were defined. In addition, each component was critically accessed regarding its recyclability and target elements.

With the knowledge of the structure of a PEMWE stack from the first part, a conceptual outline of a combined mechanical and hydrometallurgical recycling chain could then be developed. This includes the dismantling of the stack, followed by mechanical processing, including MEA/CCM shredding, sorting, CCM decoating, CCM dissolution, and anode and cathode separation. The precious metals from the catalysts are then recovered hydro metallurgically. Finally, the carbon from the cathode can be reused.

Some of these process steps have been investigated independently on model material proving their application. During disassembly, adhesive joints were found that were not caused by the manufacturing process, but by the operation of the electrolyzer at high pressures. These joints can be separated by an automated non-destructive cutting tool. Dry mechanical decoating of the CCM showed that the electrode layers can be liberated from the membrane material by mechanical stress. Depending on the type of CCM and the electrode side, up to 99 % decoating efficiency was achieved. An alternative to get access to the membrane coating of the CCM is to dissolve the CCM at high temperatures and pressures, which enables to recover the valuable membrane material as an ionomer dispersion. More than 99 % of iridium and platinum recovery has been achieved in small scale experiments.

Once the electrodes are liberated from the membrane, a separation process based on the wetting properties of the mixed materials can be used to separate the iridium-containing anode from the platinum-containing cathode material.

For the platinum-containing catalyst on the cathode side, standard metallurgical processes are available to dissolve the platinum with very high efficiency. However, these involve highly corrosive chemicals, so a more environmentally friendly alternative was sought and tested on carbon-supported platinum. Using hydrochloric acid in combination with organic acids and other oxidizing agent and salts, leaching efficiencies of > 70 % can be achieved even before optimization.

These individual highlights, some of which have been tested on model material, still need to be validated on real EoL electrolyzer material and scaled up from small and laboratory to pilot and production scale. In addition, the entire process chain needs to be validated in sequence, which would require a PEMWE stack to be processed through all steps of the entire chain. These results can then be used to calculate element-specific recoveries, which can also be used for life cycle assessment and techno-economic assessment.

Abbreviations

The following abbreviations are used in this manuscript:

BPP	Bipolar plates
CCM	Catalyst coated membrane
EoL	End of life
GDL	gas diffusion layer
LGDL	liquid gas diffusion layers
LLPS	Liquid-liquid phase/particle separation
PEM	Proton exchange membrane
PEMFC	PEM fuel cell
PEMWE	PEM water electrolyzers
PGM	Platin group metal
PFSA	perfluorosulfonic acid
PTE	porous transport electrodes
PTFE	polytetrafluoroethylene
PTL	Porous transport layer
μXRF	Micro X-ray fluorescence spectroscopy

References

1. IEA. *Global Hydrogen Review 2023*; Paris, 2023.

2. C. Hebling, M.R., T. Fleiter, U. Groos, D. Härle, A. Held, M. Jahn, N. Müller, T. Pfeifer, P. Plötz, O. Ranzmeyer, A. Schaadt, F. Sensfuß, T. Smolinka, M. Wietschel. *Eine Wasserstoff-Roadmap für Deutschland*; Fraunhofer-Institut für System- und Innovationsforschung ISI, Karlsruhe; Fraunhofer-Institut für Solare Energiesysteme ISE, Freiburg; unter Beteiligung von Fraunhofer-Institut für Mikrostruktur von Werkstoffen und Systemen IMWS, Halle; Fraunhofer-Institut für Keramische Technologien und Systeme IKTS, Dresden: Karlsruhe, Freiburg, 2019.

3. Minke, C.; Suermann, M.; Bensmann, B.; Hanke-Rauschenbach, R. Is iridium demand a potential bottleneck in the realization of large-scale PEM water electrolysis? *International Journal of Hydrogen Energy* **2021**, *46*, 23581-23590, doi: 10.1016/j.ijhydene.2021.04.174.

4. Carmo, M.; Fritz, D.L.; Mergel, J.; Stolten, D. A comprehensive review on PEM water electrolysis. *International Journal of Hydrogen Energy* **2013**, *38*, 4901-4934, doi: 10.1016/j.ijhydene.2013.01.151.

5. Shiva Kumar, S.; Himabindu, V. Hydrogen production by PEM water electrolysis – A review. *Materials Science for Energy Technologies* **2019**, *2*, 442-454, doi: 10.1016/j.mset.2019.03.002.

6. Bernt, M.; Schröter, J.; Möckl, M.; Gasteiger, H.A. Analysis of Gas Permeation Phenomena in a PEM Water Electrolyzer Operated at High Pressure and High Current Density. *Journal of The Electrochemical Society* **2020**, *167*, 124502, doi: 10.1149/1945-7111/abaa68.

7. Moschovi, A.M.; Zagoraiou, E.; Polyzou, E.; Yakoumis, I. Recycling of Critical Raw Materials from Hydrogen Chemical Storage Stacks (PEMWE), Membrane Electrode Assemblies (MEA) and Electrocatalysts. *IOP Conference Series: Materials Science and Engineering* **2021**, *1024*, 012008, doi: 10.1088/1757-899x/1024/1/012008.

8. Aricò, A.S.; Siracusano, S.; Briguglio, N.; Baglio, V.; Di Blasi, A.; Antonucci, V. Polymer electrolyte membrane water electrolysis: status of technologies and potential applications in combination with renewable power sources. *Journal of Applied Electrochemistry* **2013**, *43*, 107-118, doi: 10.1007/s10800-012-0490-5.

9. Bareiß, K.; de la Rua, C.; Möckl, M.; Hamacher, T. Life cycle assessment of hydrogen from proton exchange membrane water electrolysis in future energy systems. *Applied Energy* **2019**, *237*, 862-872, doi: 10.1016/j.apenergy.2019.01.001.

10. Valente, A.; Martín-Gamboa, M.; Iribarren, D.; Dufour, J. *Deliverable 2.2 Existing end-of-life technologies applicable to FCH products*; 2016.

11. Mo, J.; Steen, S.; Han, B.; Kang, Z.; Terekhov, A.; Zhang, F.-Y.; Retterer, S.T.; Cullen, D.A. Investigation of titanium felt transport parameters for energy storage and hydrogen/oxygen production. In Proceedings of the 13th International Energy Conversion Engineering Conference, Orlando, FL, 2015.

12. Toray. Torayca® Carbon Paper for Fuel Cells. Available online: https://toray-cfe.com/en/products/carbon-paper/ (accessed on 29.02.2024).

13. TANAKA Precious Metals. Electrocatalysts for Fuel Cell / Water Electrolysis (PEM type). Available online: https://tanaka-preciousmetals.com/en/products/detail/pefcs/?nav=func (accessed on 09.09.2024).

14. Mott. Porous Transport Layers for Electrolysis. Available online: https://mottcorp.com/product/gas-diffusion-transport-layers/porous-transport-layers/#:~:text=For%20customers%20working%20on%20electrolysis,resistance%20to%20bending%20and%20cracking (accessed on 29.02.2024).

15. GORE. GORE® PEM for Water electrolysis. Available online: https://www.gore.com/system/files/2024-02/GORE-PEM-Water-Electrolysis-Datasheet-EN.pdf (accessed on 29.02.2024).

16. Freudenberg. Freundenberg Gas Diffusion Layers - Technical data. Available online: https://www.fuelcellstore.com/spec-sheets/freudenberg-gdl-technical-data.pdf (accessed on 29.02.2024).

17. fumatech. Membranes for PEM water electrolysis (PEMWE)). Available online: https://www.fumatech.com/en/products/membranes-pem-water-electrolysis/ (accessed on 29.02.2024).

18. DuPontTM. Nafion® PFSA Membranes - Product information. Available online: http://www.hesen.cn/userfiles/bochi/file/117%E3%80%81115%E5%8F%82%E6%95%B0.pdf (accessed on 29.02.2024).

19. SGL CARBON. SIGRACET® Fuel Cell Components. Available online: https://www.sglcarbon.com/data/pdf/SIGRACET-Whitepaper.pdf; https://www.sglcarbon.com/en/markets-solutions/material/sigracet-fuel-cell-components/ (accessed on 29.02.2024).

20. Holzapfel, P.; Bühler, M.; Van Pham, C.; Hegge, F.; Böhm, T.; McLaughlin, D.; Breitwieser, M.; Thiele, S. Directly coated membrane electrode assemblies for proton exchange membrane water electrolysis. *Electrochemistry Communications* **2020**, *110*, doi: 10.1016/j.elecom.2019.106640.

21. Valente, A.; Iribarren, D.; Dufour, J. End of life of fuel cells and hydrogen products: From technologies to strategies. *International Journal of Hydrogen Energy* **2019**, *44*, 20965-20977, doi: 10.1016/j.ijhydene.2019.01.110.

22. Steinmüller, H.; Tichler, R.; Reiter, G.; Koppe, M.; Harasek, M.; Haider, M.; Gawlik, W.; Haas, R. *Power to Gas – eine Systemanalyse. Markt- und Technologiescouting und -analyse (Endbericht 2014)*; 2014.

23. Chatterjee, S.; Peng, X.; Intikhab, S.; Zeng, G.; Kariuki, N.N.; Myers, D.J.; Danilovic, N.; Snyder, J. Nanoporous Iridium Nanosheets for Polymer Electrolyte Membrane Electrolysis. *Advanced Energy Materials* **2021**, *11*, 2101438, doi: 10.1002/aenm.202101438.

24. Taie, Z.; Peng, X.; Kulkarni, D.; Zenyuk, I.V.; Weber, A.Z.; Hagen, C.; Danilovic, N. Pathway to Complete Energy Sector Decarbonization with Available Iridium Resources using Ultralow Loaded Water Electrolyzers. *ACS Applied Materials & Interfaces* **2020**, *12*, 52701-52712, doi: 10.1021/acsami.0c15687.

25. Mirshekari, G.; Ouimet, R.; Zeng, Z.; Yu, H.; Bliznakov, S.; Bonville, L.; Niedzwiecki, A.; Capuano, C.; Ayers, K.; Maric, R. High-performance and cost-effective membrane electrode assemblies for advanced proton exchange membrane water electrolyzers: Long-term durability assessment. *International Journal of Hydrogen Energy* **2021**, *46*, 1526-1539, doi: 10.1016/j.ijhydene.2020.10.112.

26. Yu, H.; Bonville, L.; Jankovic, J.; Maric, R. Microscopic insights on the degradation of a PEM water electrolyzer with ultra-low catalyst loading. *Applied Catalysis B: Environmental* **2020**, *260*, doi: 10.1016/j.apcatb.2019.118194.

27. Rozain, C.; Mayousse, E.; Guillet, N.; Millet, P. Influence of iridium oxide loadings on the performance of PEM water electrolysis cells: Part II – Advanced oxygen electrodes. *Applied Catalysis B: Environmental* **2016**, *182*, 123-131, doi: 10.1016/j.apcatb.2015.09.011.

28. Ayers, K.; Danilovic, N.; Ouimet, R.; Carmo, M.; Pivovar, B.; Bornstein, M. Perspectives on Low-Temperature Electrolysis and Potential for Renewable Hydrogen at Scale. *Annual Review of Chemical and Biomolecular Engineering* **2019**, *10*, 219-239, doi: 10.1146/annurev-chembioeng-060718-030241.

29. Su, H.; Linkov, V.; Bladergroen, B.J. Membrane electrode assemblies with low noble metal loadings for hydrogen production from solid polymer electrolyte water electrolysis. *International Journal of Hydrogen Energy* **2013**, *38*, 9601-9608, doi: 10.1016/j.ijhydene.2013.05.099.

30. Pantò, F.; Siracusano, S.; Briguglio, N.; Aricò, A.S. Durability of a recombination catalyst-based membrane-electrode assembly for electrolysis operation at high current density. *Applied Energy* **2020**, *279*, 115809, doi: 10.1016/j.apenergy.2020.115809.

31. Xu, W.; Scott, K. The effects of ionomer content on PEM water electrolyser membrane electrode assembly performance. *International Journal of Hydrogen Energy* **2010**, *35*, 12029-12037, doi: 10.1016/j.ijhydene.2010.08.055.

32. Pham, C.V.; Escalera-López, D.; Mayrhofer, K.; Cherevko, S.; Thiele, S. Essentials of High Performance Water Electrolyzers – From Catalyst Layer Materials to Electrode Engineering. *Advanced Energy Materials* **2021**, *11*, 2101998, doi: 10.1002/aenm.202101998.

33. Bernt, M.; Siebel, A.; Gasteiger, H.A. Analysis of Voltage Losses in PEM Water Electrolyzers with Low Platinum Group Metal Loadings. *Journal of The Electrochemical Society* **2018**, *165*, F305-F314, doi: 10.1149/2.0641805jes.

34. Padgett, E.; Bender, G.; Haug, A.; Lewinski, K.; Sun, F.; Yu, H.; Cullen, D.A.; Steinbach, A.J.; Alia, S.M. Catalyst Layer Resistance and Utilization in PEM Electrolysis. *Journal of The Electrochemical Society* **2023**, *170*, 084512, doi: 10.1149/1945-7111/acee25.

35. Grigoriev, S.A.; Millet, P.; Fateev, V.N. Evaluation of carbon-supported Pt and Pd nanoparticles for the hydrogen evolution reaction in PEM water electrolysers. *Journal of Power Sources* **2008**, *177*, 281-285, doi: 10.1016/j.jpowsour.2007.11.072.

36. Wang, W.; Wang, Z.; Wang, J.; Zhong, C.-J.; Liu, C.-J. Highly Active and Stable Pt-Pd Alloy Catalysts Synthesized by Room-Temperature Electron Reduction for Oxygen Reduction Reaction. *Advanced Science* **2017**, *4*, 1600486, doi: 10.1002/advs.201600486.

37. Deutsche Rohstoffagentur (DERA) in der Bundesanstalt für Geowissenschaften und Rohstoffe (BGR). *Preismonitor Dezember 2024*; 2024.

38. Stähler, M.; Stähler, A.; Scheepers, F.; Carmo, M.; Lehnert, W.; Stolten, D. Impact of porous transport layer compression on hydrogen permeation in PEM water electrolysis. *International Journal of Hydrogen Energy* **2020**, *45*, 4008-4014, doi: 10.1016/j.ijhydene.2019.12.016.

39. Briguglio, N.; Pantò, F.; Siracusano, S.; Aricò, A.S. Enhanced performance of a PtCo recombination catalyst for reducing the H2 concentration in the O2 stream of a PEM electrolysis cell in the presence of a thin membrane and a high differential pressure. *Electrochimica Acta* **2020**, *344*, 136153, doi: 10.1016/j.electacta.2020.136153.

40. Wittstock, R.; Pehlken, A.; Wark, M. Challenges in Automotive Fuel Cells Recycling. *Recycling* **2016**, *1*, 343-364, doi: 10.3390/recycling1030343.

41. Lettenmeier, P. Entwicklung und Integration neuartiger Komponenten für Polymerelektrolytmembran-(PEM) Elektrolyseure. Dissertation, Universität Stuttgart, Stuttgart, 2018.

42. Inamuddin, D.; Mohammad, A.; Asiri, A.M. *Organic-Inorganic Composite Polymer Electrolyte Membranes: Preparation, Properties, and Fuel Cell Applications*; Springer International Publishing: Cham, 2017.

43. Klose, C.; Saatkamp, T.; Münchinger, A.; Bohn, L.; Titvinidze, G.; Breitwieser, M.; Kreuer, K.D.; Vierrath, S. All-Hydrocarbon MEA for PEM Water Electrolysis Combining Low Hydrogen Crossover and High Efficiency. *Advanced Energy Materials* **2020**, *10*, doi: 10.1002/aenm.201903995.

44. Bessarabov, D. (Invited) Membranes with Recombination Catalyst for Hydrogen Crossover Reduction: Water Electrolysis. *ECS Transactions* **2018**, *85*, 17-25, doi: 10.1149/08511.0017ecst.

45. Trinke, P.; Haug, P.; Brauns, J.; Bensmann, B.; Hanke-Rauschenbach, R.; Turek, T. Hydrogen Crossover in PEM and Alkaline Water Electrolysis: Mechanisms, Direct Comparison and Mitigation Strategies. *Journal of The Electrochemical Society* **2018**, *165*, F502-F513, doi: 10.1149/2.0541807jes.

46. Ma, L.; Zimmerer, N.; Schäfer, J.; Quarz, P.; Heckmann, T.; Scharfer, P.; Schabel, W.; Fleischer, J. Investigation on a micro-environment concept for MEA production process supported by numerical simulations. In Proceedings of the FC³ - 2nd Fuel Cell Conference Chemnitz 2022 - Saubere Antriebe. Effizient Produziert. : Wissenschaftliche Beiträge und Präsentationen der zweiten Brennstoffzellenkonferenz am 31. Mai und 01. Juni 2022 in Chemnitz. Hrsg.: Thomas von Unwerth, Welf-Guntram Drossel, Chemnitz, Deutschland, 2022.

47. Kusoglu, A.; Weber, A.Z. New Insights into Perfluorinated Sulfonic-Acid Ionomers. *Chemical Reviews* **2017**, *117*, 987-1104, doi: 10.1021/acs.chemrev.6b00159.

48. Wu, X.; Scott, K.; Puthiyapura, V. Polymer electrolyte membrane water electrolyser with Aquivion® short side chain perfluorosulfonic acid ionomer binder in catalyst layers. *International Journal of Hydrogen Energy* **2012**, *37*, 13243-13248, doi: 10.1016/j.ijhydene.2012.06.093.

49. Carmo, M.; Keeley, G.P.; Holtz, D.; Grube, T.; Robinius, M.; Müller, M.; Stolten, D. PEM water electrolysis: Innovative approaches towards catalyst separation, recovery and recycling. *International Journal of Hydrogen Energy* **2019**, *44*, 3450-3455, doi: 10.1016/j.ijhydene.2018.12.030.

50. Alipour Moghaddam, J.; Parnian, M.J.; Rowshanzamir, S. Preparation, characterization, and electrochemical properties investigation of recycled proton exchange membrane for fuel cell applications. *Energy* **2018**, *161*, 699-709, doi: 10.1016/j.energy.2018.07.123.

51. Kutter, M.; Greve, C.; Maier, M.; Schilling, M.; Mauel, A.; Hilgert, A.; Hoffmann, H.; Hagemeier, W.; Rosin, A.; Muggli, M.; et al. Recycling of perfluorosulfonic acid-based membranes and their Re-application in PEM fuel cells. *Journal of Membrane Science* **2024**, *693*, 122370, doi: 10.1016/j.memsci.2023.122370.

52. Hoh, M.A. Poröse Transportschichten für die Polymerelektrolytmembran-Wasserelektrolyse. Dissertation, RWTH Aachen University, Jülich, 2017.

53. Liu, C.; Shviro, M.; Gago, A.S.; Zaccarine, S.F.; Bender, G.; Gazdzicki, P.; Morawietz, T.; Biswas, I.; Rasinski, M.; Everwand, A.; et al. Exploring the Interface of Skin-Layered Titanium Fibers for Electrochemical Water Splitting. *Advanced Energy Materials* **2021**, *11*, doi: 10.1002/aenm.202002926.

54. Maier, M.; Smith, K.; Dodwell, J.; Hinds, G.; Shearing, P.R.; Brett, D.J.L. Mass transport in PEM water electrolysers: A review. *International Journal of Hydrogen Energy* **2022**, *47*, 30-56, doi: 10.1016/j.ijhydene.2021.10.013.

55. Borgardt, E.; Panchenko, O.; Hackemüller, F.J.; Giffin, J.; Bram, M.; Müller, M.; Lehnert, W.; Stolten, D. Mechanical characterization and durability of sintered porous transport layers for polymer electrolyte membrane electrolysis. *Journal of Power Sources* **2018**, *374*, 84-91, doi: 10.1016/j.jpowsour.2017.11.027.

56. Borgardt, E. Mechanische Eigenschaften von katalysatorbeschichteten Membranen für die Polymer-Elektrolyt-Membran Elektrolyse. Dissertation, RWTH Aachen, Jülich, 2021.

57. Zhang, K.; Liang, X.; Wang, L.; Sun, K.; Wang, Y.; Xie, Z.; Wu, Q.; Bai, X.; Hamdy, M.S.; Chen, H.; et al. Status and perspectives of key materials for PEM electrolyzer. *Nano Research Energy* **2022**, *1*, e9120032, doi: 10.26599/NRE.2022.9120032.

58. Shirvanian, P.; van Berkel, F. Novel components in Proton Exchange Membrane (PEM) Water Electrolyzers (PEMWE): Status, challenges and future needs. A mini review. *Electrochemistry Communications* **2020**, *114*, doi: 10.1016/j.elecom.2020.106704.

59. Bekaert. Porous transport layers for electrochemical production of hydrogen and green molecules. Available online: https://www.bekaert.com/en/product-catalog/metal-fibers/engineered-solutions/porous-transport-layers (accessed on 29.02.2024).

60. Rakousky, C.; Reimer, U.; Wippermann, K.; Carmo, M.; Lueke, W.; Stolten, D. An analysis of degradation phenomena in polymer electrolyte membrane water electrolysis. *Journal of Power Sources* **2016**, *326*, 120-128, doi: 10.1016/j.jpowsour.2016.06.082.

61. Kurzweil, P.; Dietlmeier, O.K. *Elektrochemische Speicher*, 1 ed.; Springer Vieweg: Wiesbaden, 2015; pp. XIX, 579.

62. Grigoriev, S.A.; Millet, P.; Volobuev, S.A.; Fateev, V.N. Optimization of porous current collectors for PEM water electrolysers. *International Journal of Hydrogen Energy* **2009**, *34*, 4968-4973, doi: https://doi.org/10.1016/j.ijhydene.2008.11.056.

63. Panchenko, O.; Carmo, M.; Rasinski, M.; Arlt, T.; Manke, I.; Müller, M.; Lehnert, W. Non-destructive in-operando investigation of catalyst layer degradation for water electrolyzers using synchrotron radiography. *Materials Today Energy* **2020**, *16*, 100394, doi: 10.1016/j.mtener.2020.100394.

64. Bach, M.; Gehre, P.; Biermann, H.; Aneziris, C.G. Recycling of carbon fiber composites in carbon-bonded alumina refractories. *Ceramics International* **2020**, *46*, 12574-12583, doi: 10.1016/j.ceramint.2020.02.020.

65. Stähler, A.; Stähler, M.; Scheepers, F.; Lehnert, W.; Carmo, M. Scalable Implementation of Recombination Catalyst Layers to Mitigate Gas Crossover in PEM Water Electrolyzers. *Journal of the Electrochemical Society* **2022**, *169*, doi: 10.1149/1945-7111/ac5c9b.

66. cmc Klebetechnik. Adhesive film for PEM fuel cells and PEM electrolysis cells. Available online: https://www.cmc.de/en/wasserstofftechnik-brennstoffzellen (accessed on 29.02.2024).

67. Mayyas, A.T.; Ruth, M.; Pivovar, B.S.; Bender, G.; Wipke, K.B. *Manufacturing Cost Analysis for Proton Exchange Membrane Water Electrolyzers*; United States, 2019.

68. Langemann, M.; Fritz, D.L.; Müller, M.; Stolten, D. Validation and characterization of suitable materials for bipolar plates in PEM water electrolysis. *International Journal of Hydrogen Energy* **2015**, *40*, 11385-11391, doi: 10.1016/j.ijhydene.2015.04.155.

69. Teuku, H.; Alshami, I.; Goh, J.; Masdar, M.S.; Loh, K.S. Review on bipolar plates for low-temperature polymer electrolyte membrane water electrolyzer. *International Journal of Energy Research* **2021**, *45*, 20583-20600, doi: 10.1002/er.7182.

70. Kellenberger, A.; Vaszilcsin, N.; Duca, D.; Dan, M.L.; Duteanu, N.; Stiber, S.; Morawietz, T.; Biswas, I.; Ansar, S.A.; Gazdzicki, P.; et al. Towards Replacing Titanium with Copper in the Bipolar Plates for Proton Exchange Membrane Water Electrolysis. *Materials* **2022**, *15*, doi:10.3390/ma15051628.

71. Moreno Soriano, R.; Rojas, N.; Nieto, E.; de Guadalupe González-Huerta, R.; Sandoval-Pineda, J.M. Influence of the gasket materials on the clamping pressure distribution in a PEM water electrolyzer: Bolt torques and operation mode in pre-conditioning. *International Journal of Hydrogen Energy* **2021**, *46*, 25944-25953, doi: 10.1016/j.ijhydene.2021.03.076.

72. Höller, S. Water electrolysis stack for generating hydrogen and oxygen from water. 2022.

73. Selamet, Ö.F.; Acar, M.C.; Mat, M.D.; Kaplan, Y. Effects of operating parameters on the performance of a high-pressure proton exchange membrane electrolyzer. *International Journal of Energy Research* **2013**, *37*, 457-467, doi: 10.1002/er.2942.

74. Borgardt, E.; Giesenberg, L.; Reska, M.; Müller, M.; Wippermann, K.; Langemann, M.; Lehnert, W.; Stolten, D. Impact of clamping pressure and stress relaxation on the performance of different polymer electrolyte membrane water electrolysis cell designs. *International Journal of Hydrogen Energy* **2019**, *44*, 23556-23567, doi: 10.1016/j.ijhydene.2019.07.075.

75. Hydrogen Europe. *Hydrogen Europe Position Paper on PFAS*; 2023.

76. Selamet, O.F.; Ergoktas, M.S. Effects of bolt torque and contact resistance on the performance of the polymer electrolyte membrane electrolyzers. *Journal of Power Sources* **2015**, *281*, 103-113, doi: 10.1016/j.jpowsour.2015.01.162.

77. Smolinka, T.; Lehner, F.; Kiemel, S. *Studie IndWEDe - Industrialisierung der Wasserelektrolyse in Deutschland: Chancen und Herausforderungen für nachhaltigen Wasserstoff für Verkehr, Strom und Wärme*; Nationale Organisation Wasserstoff- und Brennstoffzellentechnologie – NOW GmbH: Berlin, 2018.

78. Caparrós Mancera, J.J.; Segura Manzano, F.; Andújar, J.M.; Vivas, F.J.; Calderón, A.J. An Optimized Balance of Plant for a Medium-Size PEM Electrolyzer: Design, Control and Physical Implementation. *Electronics* **2020**, *9*, doi: 10.3390/electronics9050871.

79. Selamet, Ö.F.; Becerikli, F.; Mat, M.D.; Kaplan, Y. Development and testing of a highly efficient proton exchange membrane (PEM) electrolyzer stack. *International Journal of Hydrogen Energy* **2011**, *36*, 11480-11487, doi: 10.1016/j.ijhydene.2011.01.129.

80. Siracusano, S.; Baglio, V.; Di Blasi, A.; Briguglio, N.; Stassi, A.; Ornelas, R.; Trifoni, E.; Antonucci, V.; Aricò, A.S. Electrochemical characterization of single cell and short stack PEM electrolyzers based on a nanosized IrO2 anode electrocatalyst. *International Journal of Hydrogen Energy* **2010**, *35*, 5558-5568, doi: 10.1016/j.ijhydene.2010.03.102.

81. SIEMENS. *SILYZER 300 - The next paradigm of PEM electrolysis*; 2018.

82. Hoeller Electrolyzer GmbH. Unsere Entwicklungsziele. Available online: https://hoeller-electrolyzer.com/entwicklungsziele.html (accessed on 31.05.2024).

83. Bosch GmbH. Scale the production of green hydrogen: Bosch electrolysis technology and services make it possible. Available online: https://www.bosch-hydrogen-energy.com/electrolysis/?gad_source=1&gclid=Cj0KCQjwgJyyBhCGARIsAK8LVLNkwVDiuv_y2fzD6JzVD6E6at1OqbFjd4dpPBd7FNKI067iIfsk9SQaAgTvEALw_wcB (accessed on 31.05.2024).

84. *Directive 2008/98/EC of the European Parliament and of the Council of 19 November 2008 on waste and repealing certain Directives*; 2008.

85. Al Assadi, A.; Goes, D.; Baazouzi, S.; Staudacher, M.; Malczyk, P.; Kraus, W.; Nägele, F.; Huber, M.F.; Fleischer, J.; Peuker, U.; et al. Challenges and prospects of automated disassembly of fuel cells for a circular economy. *Resources, Conservation & Recycling Advances* **2023**, *19*, 200172, doi: 10.1016/j.rcradv.2023.200172.

86. Martens, H.; Goldmann, D. *Recyclingtechnik*; Springer Vieweg Wiesbaden: 2016; pp. XXIII, 556.

87. Kumar, A.; Holuszko, M.; Espinosa, D.C.R. E-waste: An overview on generation, collection, legislation and recycling practices. *Resources, Conservation and Recycling* **2017**, *122*, 32-42, doi: 10.1016/j.resconrec.2017.01.018.

88. Werner, D.; Peuker, U.A.; Mütze, T. Recycling Chain for Spent Lithium-Ion Batteries. *Metals* **2020**, *10*, 316, doi: 10.3390/met10030316.

89. Haque, N.; Giddey, S.; Saha, S.; Sernia, P. Recyclability of Proton Exchange Membrane Electrolysers for Green Hydrogen Production. In Proceedings of the New Directions in Mineral Processing, Extractive Metallurgy, Recycling and Waste Minimization, Cham, 2023, 2023; pp. 137-150.

90. Melke, J.; Maletzko, A.; Gomez Villa, E.D.; Bornet, A.; Wiberg, G.K.H.; Arenz, M.; Sandig-Predzymirska, L.; Thiere, A.; Charitos, A.; Stelter, M.; et al. Recyclyse – New Sustainable and Recyclable Catalytic Materials for Proton Exchange Membrane Electrolysers. *Chemie Ingenieur Technik* **2024**, *96*, 126-142, doi: 10.1002/cite.202300143.

91.   Hanisch, C.; Loellhoeffel, T.; Diekmann, J.; Markley, K.J.; Haselrieder, W.; Kwade, A. Recycling of lithium-ion batteries: a novel method to separate coating and foil of electrodes. *Journal of Cleaner Production* **2015**, *108*, 301-311, doi: 10.1016/j.jclepro.2015.08.026.

92.   Werner, D.M.; Mütze, T.; Peuker, U.A. Influence of Pretreatment Strategy on the Crushing of Spent Lithium-Ion Batteries. *Metals* **2022**, *12*, 1839, doi: 10.3390/met12111839.

93.   Vanegas, P.; Peeters, J.R.; Cattrysse, D.; Tecchio, P.; Ardente, F.; Mathieux, F.; Dewulf, W.; Duflou, J.R. Ease of disassembly of products to support circular economy strategies. *Resources, Conservation and Recycling* **2018**, *135*, 323-334, doi: 10.1016/j.resconrec.2017.06.022.

94.   Khatib, F.N.; Wilberforce, T.; Ijaodola, O.; Ogungbemi, E.; El-Hassan, Z.; Durrant, A.; Thompson, J.; Olabi, A.G. Material degradation of components in polymer electrolyte membrane (PEM) electrolytic cell and mitigation mechanisms: A review. *Renewable and Sustainable Energy Reviews* **2019**, *111*, 1-14, doi: 10.1016/j.rser.2019.05.007.

95.   Millet, P.; Ranjbari, A.; de Guglielmo, F.; Grigoriev, S.A.; Auprêtre, F. Cell failure mechanisms in PEM water electrolyzers. *International Journal of Hydrogen Energy* **2012**, *37*, 17478-17487, doi: 10.1016/j.ijhydene.2012.06.017.

96.   Feng, Q.; Yuan, X.Z.; Liu, G.; Wei, B.; Zhang, Z.; Li, H.; Wang, H. A review of proton exchange membrane water electrolysis on degradation mechanisms and mitigation strategies. *Journal of Power Sources* **2017**, *366*, 33-55, doi: 10.1016/j.jpowsour.2017.09.006.

97.   European Environment Agency. *Accelerating the circular economy in Europe - State and outlook 2024*; 2024.

98.   *Construction adhesives - Guideline for separation and recycling of adhesives and substrates from bonded joints. DIN/TS 54405:2020-12*; 2020.

99.   Bharti, A.; Natarajan, R. Recovery of expensive Pt/C catalysts from the end-of-life membrane electrode assembly of proton exchange membrane fuel cells. *RSC Advances* **2020**, *10*, 35057-35061, doi: 10.1039/D0RA06640K.

100. Arlt, C.-R.; Brekel, D.; Franzreb, M. Continuous fractionation of nanoparticles based on their magnetic properties applying simulated moving bed chromatography. *Separation and Purification Technology* **2021**, *259*, 118123, doi: 10.1016/j.seppur.2020.118123.

101. Rhein, F.; Scholl, F.; Nirschl, H. Magnetic seeded filtration for the separation of fine polymer particles from dilute suspensions: Microplastics. *Chemical Engineering Science* **2019**, *207*, 1278-1287, doi: 10.1016/j.ces.2019.07.052.

102. Giesler, J.; Pesch, G.R.; Weirauch, L.; Schmidt, M.-P.; Thöming, J.; Baune, M. Polarizability-Dependent Sorting of Microparticles Using Continuous-Flow Dielectrophoretic Chromatography with a Frequency Modulation Method. *Micromachines* **2020**, *11*, doi:10.3390/mi11010038.

103. Ahn, S.; Rudolph, M. Development of Fine Particle Mechanical Separation Processes with Representative Catalyst Materials for Recycling PEM Water Electrolyzers Exploiting their Wetting Characteristics. *ChemCatChem* **2023**, *n/a*, e202300931, doi: 10.1002/cctc.202300931.

104. Miettinen, T.; Ralston, J.; Fornasiero, D. The limits of fine particle flotation. *Minerals Engineering* **2010**, *23*, 420-437, doi: 10.1016/j.mineng.2009.12.006.

105. Ahn, S.; Patil, S.; Rudolph, M. Ultrafine Particle Recycling—Efficiency of the Hydrophobic Double Emulsion Technique for the Selective Agglomeration and Froth Flotation of Ultrafine Cathode Catalyst Particles from PEM Water Electrolyzers. *ACS Engineering Au* **2024**, doi: 10.1021/acsengineeringau.4c00042.

106. Machunsky, S.; Peuker, U.A. Liquid-Liquid Interfacial Transport of Nanoparticles. *Physical Separation in Science and Engineering* **2007**, *2007*, 034832, doi: 10.1155/2007/34832.

107. Heilmann, C.; Ditscherlein, L.; Peuker, U.A. Influence of Hydrolyzed Metal Ions and Surfactants on the Phase Transfer of Al2O3, SiO2, and SnO2. *Langmuir* **2024**, *40*, 2543-2550, doi: 10.1021/acs.langmuir.3c02654.

108. Olbrich, W.; Kadyk, T.; Sauter, U.; Eikerling, M. Review—Wetting Phenomena in Catalyst Layers of PEM Fuel Cells: Novel Approaches for Modeling and Materials Research. *Journal of The Electrochemical Society* **2022**, *169*, 054521, doi: 10.1149/1945-7111/ac6e8b.

109. Ahn, S.; Rudolph, M. Impact of ionomer containing particles on the selective mechanical separation processes of PEM water electrolyzer recycling for PGM recovery. In Proceedings of the International Mineral Processing Congress, Washington, DC, 2024.

110. Granados-Fernández, R.; Montiel, M.A.; Díaz-Abad, S.; Rodrigo, M.A.; Lobato, J. Platinum Recovery Techniques for a Circular Economy. *Catalysts* **2021**, *11*, doi: 10.3390/catal11080937.

111. Sverdrup, H.U.; Ragnarsdottir, K.V. A system dynamics model for platinum group metal supply, market price, depletion of extractable amounts, ore grade, recycling and stocks-in-use. *Resources, Conservation and Recycling* **2016**, *114*, 130-152, doi: 10.1016/j.resconrec.2016.07.011.

112. Saguru, C.; Ndlovu, S.; Moropeng, D. A review of recent studies into hydrometallurgical methods for recovering PGMs from used catalytic converters. *Hydrometallurgy* **2018**, *182*, 44-56, doi: 10.1016/j.hydromet.2018.10.012.

113. Asamoah-Bekoe, Y. Investigation of the leaching of the platinum group metal concentrate in hydrochloric acid solution by chlorine. Thesis, University of the Witwatersrand, Johannesburg, 1998.

114. Wilkens, M.; Peuker, U.A. Grundlagen und aktuelle Entwicklungen der Filterkuchenwaschung. *Chemie Ingenieur Technik* **2012**, *84*, 1873-1884, doi: 10.1002/cite.201200095.

115. Sauer, F.; Löwer, E.; Henn, H.; Peuker, U.; Hoffner, B. Displacement Washing of Filter Cakes With a Fine Particle Top Layer. *Chemical Engineering & Technology* **2025**, *48*, e202400394, doi: 10.1002/ceat.202400394.